Am J Cancer Res 2024;14(8):3757-3772
www.ajcr.us /ISSN:2156-6976/ajcr0155128

Original Article

Sophocarpine inhibits the progression of glioblastoma via PTEN/PI3K/Akt signaling pathway

Shuqiao Xing[1,2*], Zhenrong Xiong[1,2*], Mengmeng Wang[1,2*], Yifan Li[1,3], Jiali Shi[1,2], Yiming Qian[1,2], Jia Lei[1,2], Jiamei Jia[1,2], Weiquan Zeng[1,2], Zhihui Huang[1,2], Yuanyuan Jiang[1,2]

[1]School of Pharmacy, Hangzhou Normal University, Hangzhou 311121, Zhejiang, China; [2]Key Laboratory of Elemene Class Anti-Cancer Chinese Medicines, Engineering Laboratory of Development and Application of Traditional Chinese Medicines, Collaborative Innovation Center of Traditional Chinese Medicines of Zhejiang Province, Hangzhou Normal University, Hangzhou 311121, Zhejiang, China; [3]School of Medicine, Hangzhou Normal University, Hangzhou 311121, Zhejiang, China. [*]Equal contributors.

Received December 26, 2023; Accepted August 7, 2024; Epub August 25, 2024; Published August 30, 2024

Abstract: Glioblastoma multiforme (GBM) is the most fatal primary brain tumor which lacks effective treatment drugs. Alkaloids are known as a class of potential anti-tumor agents. Sophocarpine, a tetracyclic quinazoline alkaloid derived from *Sophora alopecuroides* L., possesses several pharmacological effects including anti-tumor effects in some malignancies. However, the effect and mechanism of sophocarpine on GBM remains to be explored. In this study, based on *in vitro* experiments, we found that sophocarpine significantly inhibited the viability, proliferation and migration of GBM cells including U251 and C6 cells in a dose- and time-dependent manner. Besides, sophocarpine arrested GBM cell cycle in G0/G1 phase and induced their apoptosis. Subsequently, we found that sophocarpine upregulated the expression of PTEN, a GBM tumor suppressor, and downregulated PI3K/Akt signaling in GBM cells. Moreover, inactivating of PTEN with bpV(phen) trihydrate partially restored the anti-GBM effects of sophocarpine via PI3K/Akt signaling. Finally, sophocarpine significantly inhibited the growth of tumor both in subcutaneous and orthotopic U251 xenograft GBM model in nude mice via PTEN/PI3K/Akt axis. Taken together, these results suggested that sophocarpine impeded GBM progression via PTEN/PI3K/Akt axis both *in vitro* and *in vivo*, providing with a promising therapy for treating GBM.

Keywords: Sophocarpine, glioblastoma, cell cycle arrest, cell apoptosis, PTEN/PI3K/Akt

Introduction

Glioblastoma multiforme (GBM) is one of the most fatal types of primary brain tumors that have a poor prognosis [1]. Despite surgery, radiation therapy, chemotherapy with temozolomide and supportive care are all performed, the median overall survival for GBM patients is still only of about 15 months [2]. Thus, it is of great benefit to develop safe and effective agents for GBM patients.

Alkaloids exist as the active components in many Chinese herbal medicines and exhibit potential for natural anti-tumor drug screening. Some of them have already been used in clinic, such as vinblastine and vincristine, two bisindole alkaloids from *Vinca rosea*, and camptothecin, a pentacyclic alkaloid from *Camptotheca acuminata*. Sophocarpine is a tetracyclic quinazoline alkaloid derived from *Sophora alopecuroides* L., also known as Kudouzi, a common anti-tumor traditional Chinese medicine [3, 4]. Sophocarpine was recorded to be used for the treatment of leukemia and trophoblastic tumors in 1978 [5]. Further, in 1984, Li *et al*. found that sophocarpine had the inhibitory effects on animal tumors [6]. Subsequently, accumulating evidences have shown that sophocarpine possesses multiple pharmacological effects, such as anti-inflammatory [7, 8], anti-oxidant [9], antiviral [10, 11] and neuroprotection properties [12, 13], as well as anti-tumor effects in some malignancies [14-17]. However, it remains unknown the roles and mechanism of sophocarpine in anti-GBM.

https://doi.org/10.62347/SQJB1901

PTEN (Phosphatase and Tensin homologue deleted on chromosome Ten) was identified to function as a tumor suppressor and often deleted or mutated in different types of human cancers, especially GBM [18-21]. PTEN contains motifs homology to the protein tyrosine phosphatases [18, 19], and the functional phosphatase catalytic domain of PTEN is necessary for suppressing cell growth, migration, and focal adhesion formation in glioma [22, 23]. In addition, PTEN is a phosphoinositide 3-phosphatase to catalyze dephosphorylation specifically at the position 3 on the inositol ring of phosphatidylinositol-3, 4, 5-trisphosphate (PIP3) [24], a vital Akt activator that synthesized via phosphorylating by phosphoinositide 3-kinase (PI3K) at the same position 3 of phosphatidylinositol-4, 5-bisphosphate (PIP2) [25]. Overactivated PI3K/Akt signaling and over-accumulated PIP3 are involved in regulating cell survival and growth, accelerating the progression of various cancers [26], including GBM [27]. PTEN acts as a brake to impede the accelerating process mediated by PI3K/Akt signaling via catalyzing PIP3 back to PIP2 [28, 29]. Thus, PTEN/PI3K/Akt pathway is a promising target for GBM therapy.

In the present study, we found that sophocarpine significantly suppressed GBM cell growth by inducing GBM cell cycle arrest in G0/G1 phase and promoted their apoptosis. Sophocarpine also notably regressed the tumor growth in both subcutaneous and orthotopic transplanted GBM in mice. Molecular investigation revealed that sophocarpine upregulated PTEN expression and downregulated PI3K/Akt signaling on GBM cells. Thus, these results suggest that the anti-GBM effects of sophocarpine are mediated by PTEN/PI3K/Akt axis, providing with a promising therapy for treating GBM.

Materials and methods

Cell lines, reagents and animals

U251 human GBM cell line and C6 rat GBM cell line used in this study were gifted from Prof. Maojin Yao (Guangzhou Medical University, Guangzhou, China). In a humidified atmosphere with 5% CO_2 at 37°C, cells were cultured in DMEM supplemented with 10% FBS and 1% penicillin/streptomycin.

Stock solution of sophocarpine (A0081, CHENGDU MUST BIO-TECHNOLOGY) and bpV(phen) trihydrate (HY-122818, MedChemExpress) were prepared in DMSO and deuterium-depleted water (DDW) respectively at a concentration of 400 mM.

The BALB/c nude mice (male, 18-24 g, 6-8 weeks) were purchased from Shanghai Slac Laboratory Animal Co., Ltd. The animal experiments were conducted according to the protocols approved by Animal Care and Use Committee of Hangzhou Normal University (HSD-20210401).

Cell proliferation assay

In brief, 96-well plates were seeded with 2,000 cells per well treated with sophocarpine at different concentrations for 24 h and 48 h. Then the cells were treated with CCK-8 (A311-01/02, Vazyme Biotech Co., Ltd., Nanjing, China) at the indicated time for another 2 h incubation. The optical density of cells at 450 nm was measured by a microplate reader (Varioskan Flash, Thermo Scientific, Waltham, MA, USA). The viability of cells at indicated times was assessed by comparing the viability of cells at 0 h.

Cell colony-formation assay

In a 6-well plate, 500 cells were seeded in each well and cultured. After the cells were adapted and attached to the wall, sophocarpine was added and cultured for another one week. Colonies were stained with 0.1% crystal violet followed by fixing with 4% paraformaldehyde (PFA) and then counted.

Wound healing assay and transwell assay

To assess the migration ability of cells, wound healing and transwell assay were conducted. For wound healing assay, cells were seeded in a 12-well plate. The wound was produced by using a pipette tip when the cells were grown to 95% confluence and the culture medium was changed to DMEM supplied with 1% FBS containing different concentrations of sophocarpine. Image acquisition was taken at indicated time, and wound closure ratio was calculated. Transwell chambers (8-mm pore size; Millipore) were used in transwell assay, 2×10^4 cells in 200 μL FBS-free medium with sophocarpine in different concentrations were placed in the top chamber while the lower chamber was added with 500 μL of DMEM containing 10% FBS. The

migrated cells were fixed with 4% PFA and then stained with 0.1% crystal violet and counted.

RNA extraction and RT-PCR

Total RNA was extracted using TRIzol™ reagent (TaKaRa, AL11817A). After reverse transcription, the cDNA was used for RT-PCR. β-actin was used as the endogenous control. Primers for *PTEN* were presented as: F, 5'-TTTGAAGACCATAACCCACCAC-3'; R, 5'-ATTACACCAGTTCGTCCCTTTC-3'.

Cell cycle and cell apoptosis analysis using flow cytometry

Cell cycle staining Kit (MultiSciences, Hangzhou, China) was used according to the manufacturer's instruction. Briefly, cells from a 6 cm dish treated with or without sophocarpine were harvested and fixed overnight in ice-cold 70% ethanol at 4°C. After PBS washing, 100 μL RNase was added and incubated at 37°C for 30 min. Next, PI staining at 4°C for 30 min in the dark was performed. For cell apoptosis assay, Annexin V-FITC/PI Apoptosis Detection Kit (#A00947, MULTI SCIENCES, Hangzhou, China) was used. In brief, cells with or without sophocarpine treatment were resuspended and incubated with Annexin V-FITC and PI for 10 min and washed with PBS. In both assays, flow cytometer (CytoFLEX S, Beckman Coulter) was utilized to analyze the cells. Results were analyzed using FlowJo.

Antibodies

In this study, the primary antibodies used were anti-PH3 (ab14955, Abcam, immunofluorescent staining, 1:2,500), anti-p-Akt (#13038, CST, immunofluorescent staining, 1:1,000; western blot, 1:1,000), anti-cleaved Caspase-3 (#9661, CST, western blot, 1:1,000), anti-Bcl-2 (M1206-4, HuaBio, western blot, 1:1,000), anti-P53 (#2524S, CST, western blot, 1:1,000), anti-PTEN (ab267787, Abcam, western blot, 1:1,000), anti-PI3K (1608-70, HuaBio, western blot, 1:1,000), anti-Cyclin B1 (1508-1, HuaBio, western blot, 1:1,000), anti-CyclinD1 (#1601-31, HuaBio, western blot, 1:1,000), anti-GAPDH (#2118, CST, western blot, 1:5,000), anti-E-cadherin (#14472, CST, western blot, 1:1,000), anti-Vimentin (1610-39, HuaBio, western blot, 1:1,000), anti-Tubulin (1602-4, HuaBio, western blot, 1:1,000), anti-Akt (#2920, CST, western blot, 1:1,000). For western blot, goat anti-rabbit/mouse IgG HRP-conjugated secondary antibodies (1:10,000) from Abcam was used. For immunofluorescent staining, Alexa 546-labeled goat anti-mouse IgG secondary antibody from Thermo Fisher Scientific (1:500) was used.

Proteins extraction and western blot

RIPA lysis Buffer (P0013B, Beyotime) containing cocktail and PMSF was used to lyse cells or tissues. Immediately after ultrasonication, the protein solution was placed on ice for 30 min before being centrifugated at 14,000 g at 4°C for 15 min. The collected supernatant was boiled in Laemmli sample buffer at 100°C for 10 min. 8% SDS-PAGE was used to separate the proteins and then transferred to PVDF membrane (Life sciences, USA). The membrane was blocked with 5% skim milk-contained TBST buffer for 1 h and then incubated with primary antibodies at 4°C overnight. The membranes were washed with TBST and incubated with HRP-conjugated secondary antibodies the following day. Finally, chemiluminescence detection was carried out using the ECL detection kit (Bio-Rad, USA).

Immunofluorescence assays

Cells seeded on coverslip treated with or without sophocarpine were fixed in 4% PFA for 30 min and permeabilized with 0.1% Triton X100 in PBS for 10 min followed by blocking at room temperature for 1 h with 5% BSA in PBS. Afterwards, the cells were incubated with the primary antibodies diluted in PBS with 5% BSA at 4°C overnight. After cells were incubated with fluorescently conjugated secondary antibodies, DAPI staining was applied, and then the cells were mounted. Olympus confocal microscope (FV3000, Olympus, Japan) and Olympus SLIDEVIEW™ VS200 microscope (Olympus, Japan) were used to capture images. And images were then processed with identical settings.

Tumor model and treatment

Subcutaneous GBM tumor was established by injecting of 2×10^6 U251 cells in 100 μL DMEM into the armpits of male BALB/c nude mice subcutaneously. When the tumors reached a size of about 100 mm^3, the mice were randomly and equally divided into two groups (5 mice per

group) administrated with sophocarpine (35 mg/kg) or normal saline as a control every other day by intraperitoneal injection for two weeks. The tumor volume was monitored every two days and calculated using the formula: $Width^2 \times Length \times 0.5$. Mice were sacrificed for obtaining samples for further measurement and analysis.

For intracranial GBM tumor establishment, male BALB/c nude mice were anaesthetized and positioned in a Stereotaxic Alignment System followed by injecting 5×10^5 U251-luciferase cells in 2 μL PBS in a position of +0.6 mm Anterior/Posterior, -1.8 mm Medial/Lateral and -4.0 mm Dorsal/Ventral. One week later, mice were intraperitoneally injected with 150 mg/kg D-luciferin (40901ES03, YEASEN) and bioluminescence imaging was taken by using IVIS Spectrum system (Photon IMAGER™ OPTIMA, Biospace Lab). After confirming the tumor establishment, mice were randomly divided into two groups (5 mice per group) and were given sophocarpine (35 mg/kg) or saline as control every day by intraperitoneal injection. IVIS imaging was performed every 7 days to monitor the tumor growth. Two weeks later, mice were sacrificed to obtain samples for further analysis.

Hematoxylin-eosin (HE) staining

Frozen sections (14 μm) were stained with hematoxylin, washing with DDW and then stained with eosin. Dehydration was performed sequentially with 70%, 80%, 95% and 100% ethanol and then processed with xylene. Sections were sealed with neutral resin. Images of the sections were taken using the Olympus SLIDEVIEW™ VS200 microscope from Olympus (Olympus, Japan), and then processed.

Immunohistochemistry

After drying at 60°C and washing with PBS, the frozen sections were permeabilized and blocked for 1 h at room temperature with 0.3% Triton X-100 in 5% BSA, the sections were incubated overnight at 4°C with primary antibodies including anti-PTEN (ab267787, Abcam, 1:50) and anti-cleaved Caspase-3 (#9661, CST, 1:50). The next day, enzyme-labeled goat anti-rabbit IgG polymer was used and incubated for 1 h at room temperature after washing with PBS. To detect the signal, diaminobenzidine was used followed by hematoxylin counterstaining. Following dehydration with 75%, 95% and 100% ethanol, the sections were immersed with xylene and sealed using neutral resin. The images were taken with an Olympus SLIDEVIEW™ VS200 microscope (Olympus, Japan).

Quantification and statistical analysis

Statistical analysis was performed using GraphPad Software 8.0. Two-tailed Student's *t*-test, one-way ANOVA, two-way ANOVA or two-way RM ANOVA was used to compare differences between treated groups. Data were presented as mean ± SD. $P < 0.05$ was considered to be statistically significant.

Results

Sophocarpine inhibits the viability, proliferation and migration of GBM cells

To measure the effects of sophocarpine on GBM, we firstly examined the inhibitory effect of sophocarpine (**Figure 1A**) on the viability of GBM cells by Cell Counting Kit-8 (CCK-8) assay. As shown in **Figures 1B** and S1A, sophocarpine notably suppressed the viability of U251 and C6 cells in a dose- and time-dependent manner. The half maximal concentration was about 2 mM at 48 h in both U251 and C6 cells. Subsequently, PH3 immunostaining assay showed a reduction in the percentage of $PH3^+/DAPI^+$ cells (**Figures 1C**, **1D** and S1B, S1C). Cell colony-formation assay further determined the reduced number of cell colonies along with the increased concentration of sophocarpine both in U251 and C6 cells (**Figures 1E**, **1F** and S1D, S1E). These results indicated that sophocarpine suppressed the proliferation of GBM cells.

Metastasis is responsible for as much as 90% of cancer-associated mortality [30], so we next examined whether sophocarpine inhibited GBM cell migration. Results of wound healing assay and transwell assay showed that sophocarpine significantly inhibited the migration of U251 and C6 cells, compared with that in the control group (**Figures 1G-J** and S1F-I). Migration-related proteins Vimentin and E-cadherin were detected by western blot, and Vimentin expression was notably decreased, while E-cadherin expression was upregulated in U251 cells treat-

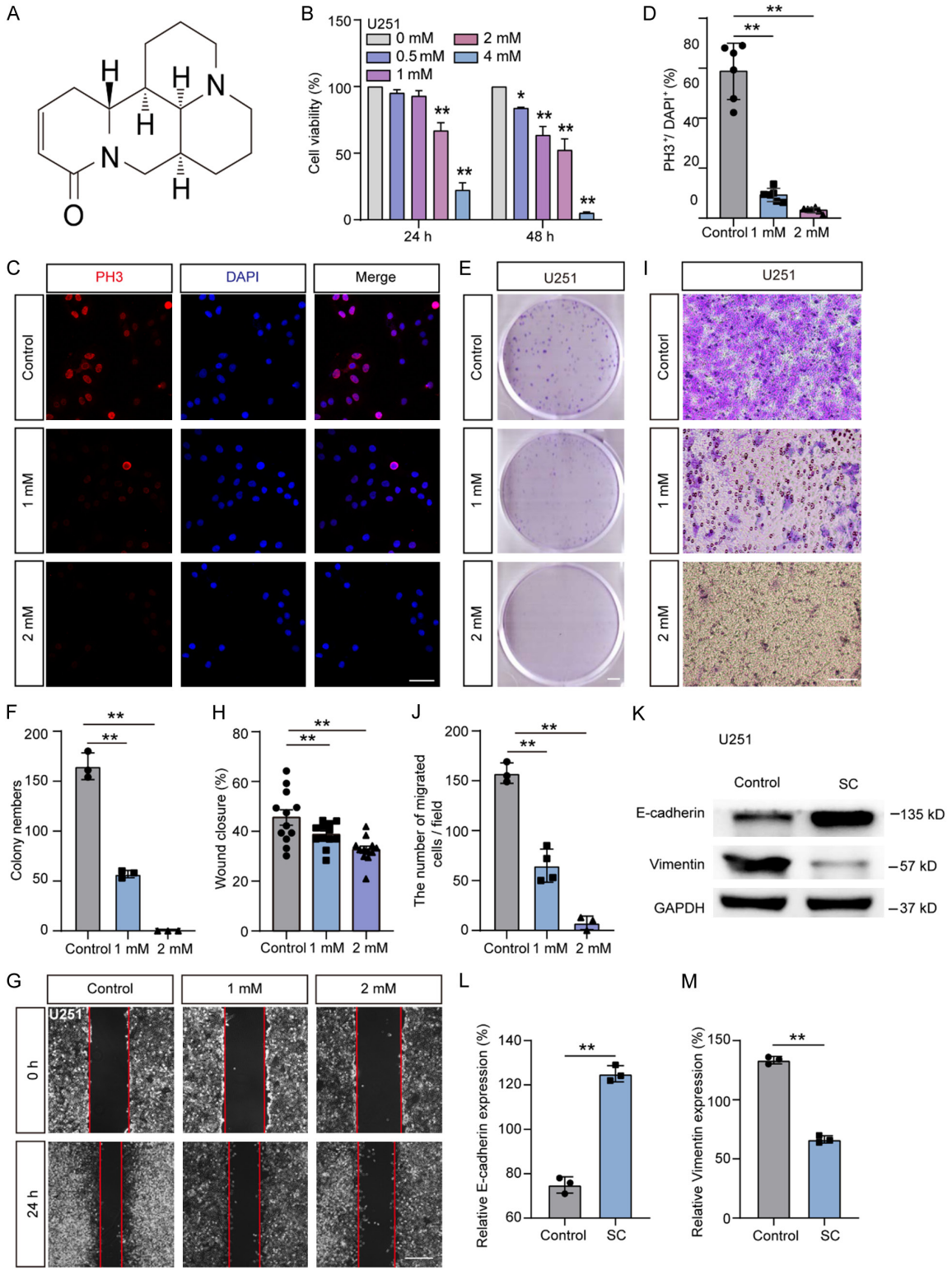

Figure 1. Sophocarpine inhibits the cell viability, proliferation and migration of U251 cells. (A) The chemical structure of sophocarpine (SC). (B) U251 cell viability upon SC concentration gradient treatment were measured by CCK8 assay (normalized to control, n=4, two-way ANOVA). (C) Immunofluorescence staining analysis of PH3 in U251 cells upon DMSO, 1 mM or 2 mM SC treatment. DAPI was labelled for nucleus. Scale bar, 50 μm. (D) Statistical analysis of the percentages of $PH3^+/DAPI^+$ cells as shown in (C) (n=6, one-way ANOVO). (E) Representative images showing the U251 cell colony formation upon DMSO, 1 mM or 2 mM SC treatment. Scale bar, 5 mm. (F) The colony numbers

were statistically analyzed as shown in (E) (n=3, one-way ANOVO). (G) Representative images showing the wound closure of U251 cells upon DMSO, 1 mM or 2 mM SC treatment. Scale bar, 150 μm. (H) Wound closure ratios were statistically analyzed as shown in (G) (n=12, one-way ANOVA). (I) Representative images of the migrated U251 cells in transwell assay upon DMSO, 1 mM or 2 mM SC treatment. Scale bar, 250 μm. (J) Statistical analysis of the migrated cells as shown in (I) (n=3, one-way ANOVO). (K) Western blot analysis of E-cadherin and Vimentin expression upon DMSO or 2 mM SC treatment in U251 cells. (L, M) Statistical analysis of the relative expression level of proteins detected in (K) (n=3, *t*-test). Data were presented as mean ± SD, $^{*}P < 0.05$; $^{**}P < 0.01$.

ed with sophocarpine (**Figure 1K-M**). These results suggested that sophocarpine inhibited the migration GBM cells.

Besides, we also performed cell viability assay on primary cultured astrocytes with the concentration gradient of sophocarpine, and the result showed that sophocarpine had no statistically significant toxicity to the primary astrocytes, thus ruling out the cytotoxicity of sophocarpine to normal cells (Figure S2).

Sophocarpine arrests GBM cell cycle at G0/G1 phase and induces the apoptosis of GBM cells

We further examined whether sophocarpine inhibited the growth of GBM cells by inducing cell cycle arrest and cell apoptosis. Flow cytometry assay showed that 2 mM sophocarpine significantly arrested cell cycle at G0/G1 phase compared with that in control-treated U251 cells (**Figure 2A**, **2B**). Western blot further showed that both Cyclin B1 and Cyclin D1 expression were downregulated in sophocarpine-treated U251 cells (**Figure 2C-E**). In addition, we noticed that U251 cells had an increased ratio of cells in subG1 (DNA content < 2N, apoptosis cells) after sophocarpine treatment (**Figure 2A**). Then we further examined the condition of sophocarpine-induced apoptosis of U251 cells with Annexin V and PI staining followed by Flow cytometry analysis. As shown in **Figure 2F**, **2G**, the proportion of apoptotic cells was significantly increased in sophocarpine-treated U251 cells. Furthermore, western blot result showed that Bcl-2, an anti-apoptosis protein, was downregulated in sophocarpine-treated U251 cells, which was accompanied with the upregulation of apoptotic executioner cleaved Caspase-3 as well as tumor suppressor P53 (**Figure 2H-K**), suggesting that sophocarpine induced the apoptosis of GBM cells via an intrinsic pathway by activating P53. Together, these results suggested that sophocarpine inhibited the growth of GBM cells by arresting cell cycle in G0/G1 phase and induced their apoptosis.

Sophocarpine upregulates PTEN and downregulates PI3K/Akt signaling in GBM cells

Previous studies have shown that loss of PTEN and hyperactivated PI3K/Akt signaling contribute to the GBM progression [26]. Consequently, we next examined if sophocarpine inhibited GBM progression via PTEN/PI3K/Akt signaling. RT-PCR was performed and showed that sophocarpine significantly upregulated *PTEN* transcription in U251 cells (**Figure 3A**). Furthermore, as expected, western blot showed that PTEN expression was significantly elevated (**Figure 3B**, **3C**) while p-Akt and Akt expression were decreased (**Figure 3B**, **3E**, **3F**), whereas PI3K level was unaffected in sophocarpine-treated U251 cells (**Figure 3B** and **3D**). Immunofluorescence staining showed that p-Akt expression was significantly decreased in sophocarpine-treated U251 cells (**Figure 3G**). These results suggested that sophocarpine upregulated PTEN expression, thus downregulated PI3K/Akt signaling in GBM cells, which might impede GBM progression.

Sophocarpine performs anti-GBM effects by upregulating PTEN and downregulating PI3K/Akt signaling

To further examine whether sophocarpine impeded GBM growth by PTEN/PI3K/Akt signaling, bpV(phen) trihydrate, a small-molecule inhibitor for PTEN [31], was used. CCK-8 results showed that bpV obviously restored the anti-viability effects on sophocarpine-treated U251 cells (**Figure 4A**). Meanwhile, bpV treatment increased the number of cell colonies as well as the percentage of $PH3^{+}$ cells in sophocarpine-treated U251 cells (**Figure 4B-E**). Furthermore, bpV significantly restored the sophocarpine's inhibitory effect on U251 cell migration detected by wound healing assay and transwell assay (**Figure 4F-I**). These results indicated that inhibition of PTEN could partially restore the inhibitory effect of sophocarpine on U251 cell viability, proliferation and migration. Furthermore, western blot was performed and

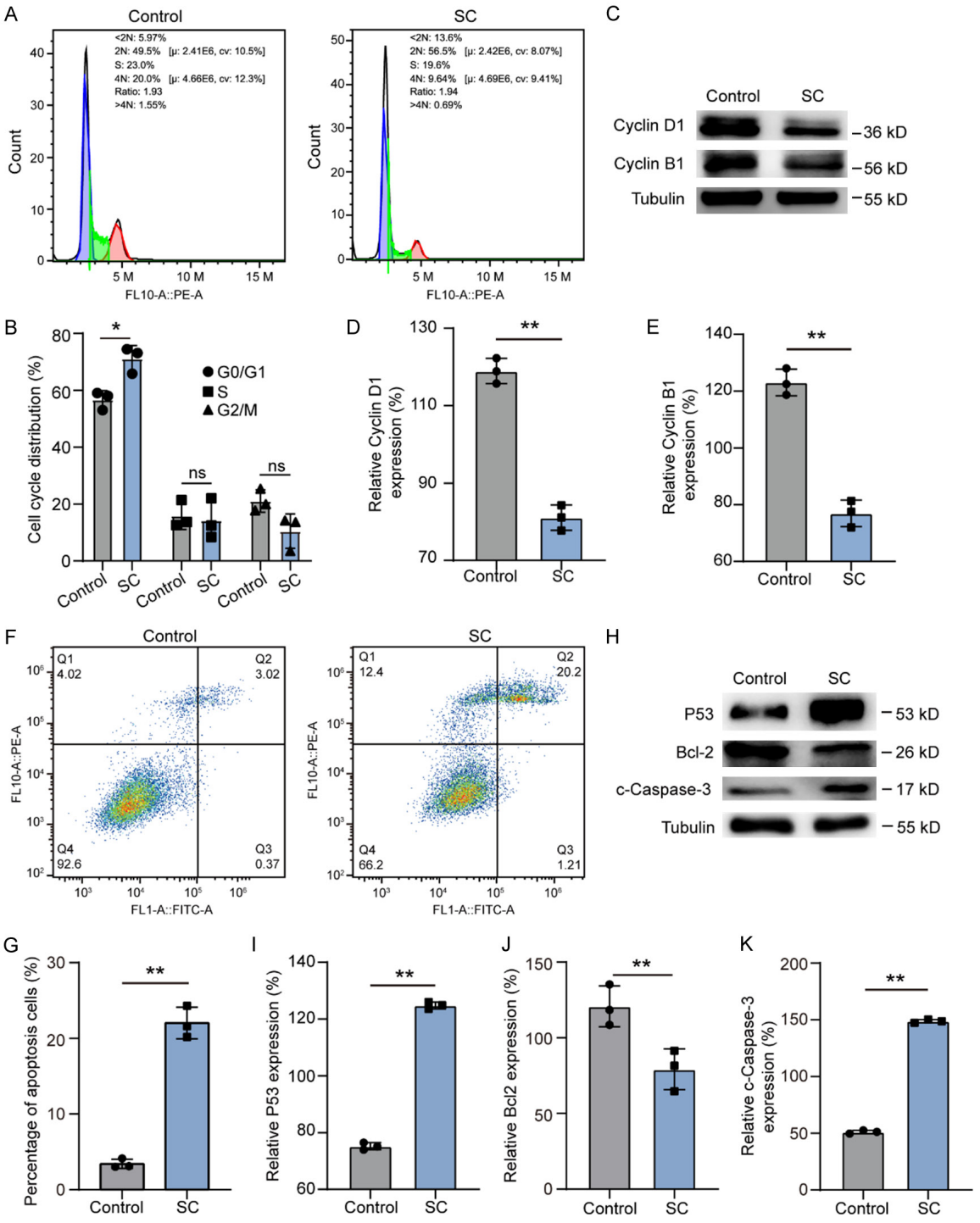

Figure 2. Sophocarpine arrests cell cycle at G0/G1 phase and induces the apoptosis of U251 cells. (A) Flow cytometry analysis of U251 cell cycle phase distribution upon DMSO or 2 mM SC treatment. (B) Statistical analysis of SC-induced cell cycle arrest shown in (A) (n=3, *t*-test). (C) Western blot analysis of Cyclin D1 and Cyclin B1 expression upon DMSO or 2 mM SC treatment in U251 cells. (D, E) Statistical analysis of the relative expression level of Cycle D1 (D) and Cyclin B1 (E) detected in (C) (n=3, *t*-test). (F) Flow cytometry analysis of the U251 cell apoptosis induced by 2 mM SC. (G) Statistical analysis of SC-induced apoptosis detected in (F) (n=3, *t*-test). (H) Western blot analysis of the p53, Bcl-2 and cleaved Caspase-3 expression of U251 cells upon DMSO or 2 mM SC treatment. (I-K) Statistical analysis of the relative expression level of proteins detected in (H) (n=3, *t*-test). Data were presented as mean ± SD, $^{*}P < 0.05$; $^{**}P < 0.01$.

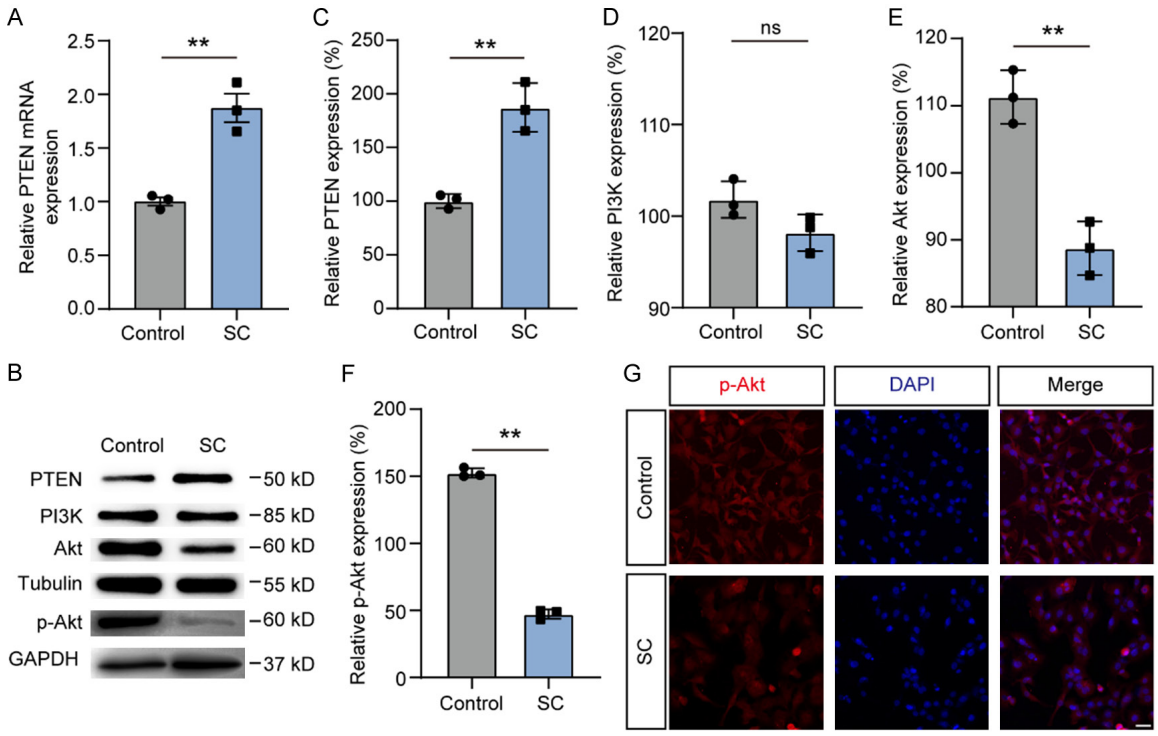

Figure 3. Sophocarpine upregulates PTEN and downregulates PI3K/Akt signaling in U251 cells. (A) RT-PCR analysis of the *PTEN* transcription of U251 cells upon DMSO or 2 mM SC treatment (normalized to control, n=3, *t*-test). (B) Western blot analysis of PTEN, PI3K, Akt and p-Akt expression of U251 cells upon DMSO or 2 mM SC treatment. (C-F) Statistical analysis of the relative expression level of proteins detected in (B) (n=3, *t*-test). (G) Immunofluorescence staining analysis of p-Akt expression in U251 cells upon DMSO or 2 mM SC treatment. Scale bar, 50 μm. Data were presented as mean ± SD, $^{**}P < 0.01$.

showed that the expression of PI3K was not influenced, while Akt was significantly upregulated in sophocarpine treated-U251 cells upon bpV treatment (**Figure 4J-M**). Overall, these results suggested that sophocarpine performed anti-GBM effects through PTEN/PI3K/Akt axis.

Sophocarpine inhibits the growth of GBM in vivo

To investigate if sophocarpine affects GBM growth *in vivo*, we first established and used a subcutaneous xenograft GBM model by injecting 2 × 10^6 U251 cells into the armpits of BALB/c nude mice. As soon as the xenografts reached about 100 mm^3, the mice were randomly divided into sophocarpine group and control group, which were respectively treated with 35 mg/kg sophocarpine or saline every two days by intraperitoneal injection for two weeks. Result showed that sophocarpine significantly inhibited GBM tumor growth (**Figure 5A**, **5B**). In comparison to control group, sophocarpine treatment showed nearly 50% reduction in tumor volume and weight without influencing the body weight of tumor-bearing mice (**Figure 5C-E**). Besides, sophocarpine-treated tumors showed the upregulated PTEN expression and downregulated Akt expression, while PI3K protein level was unchanged, which were consistent with the results *in vitro* (**Figure 5F-I**). In addition, Bcl2 was downregulated, which indicated that sophocarpine also induced cell apoptosis of GBM *in vivo* (**Figure 5F** and **5J**). Furthermore, main organs from two groups of GBM-bearing mice, including the lung, heart, liver, kidney and spleen, were collected and sectioned. Histological observation by HE staining showed no toxicity for these organs with sophocarpine treatment (Figure S3A).

Considering GBM is an intracranial tumor, so we next established a mouse orthotopic xenograft GBM model by injecting U251-luciferase cells into the brain of nude mice and examined whether sophocarpine impeded intracranial GBM growth *in vivo* (**Figure 6A**). As expected,

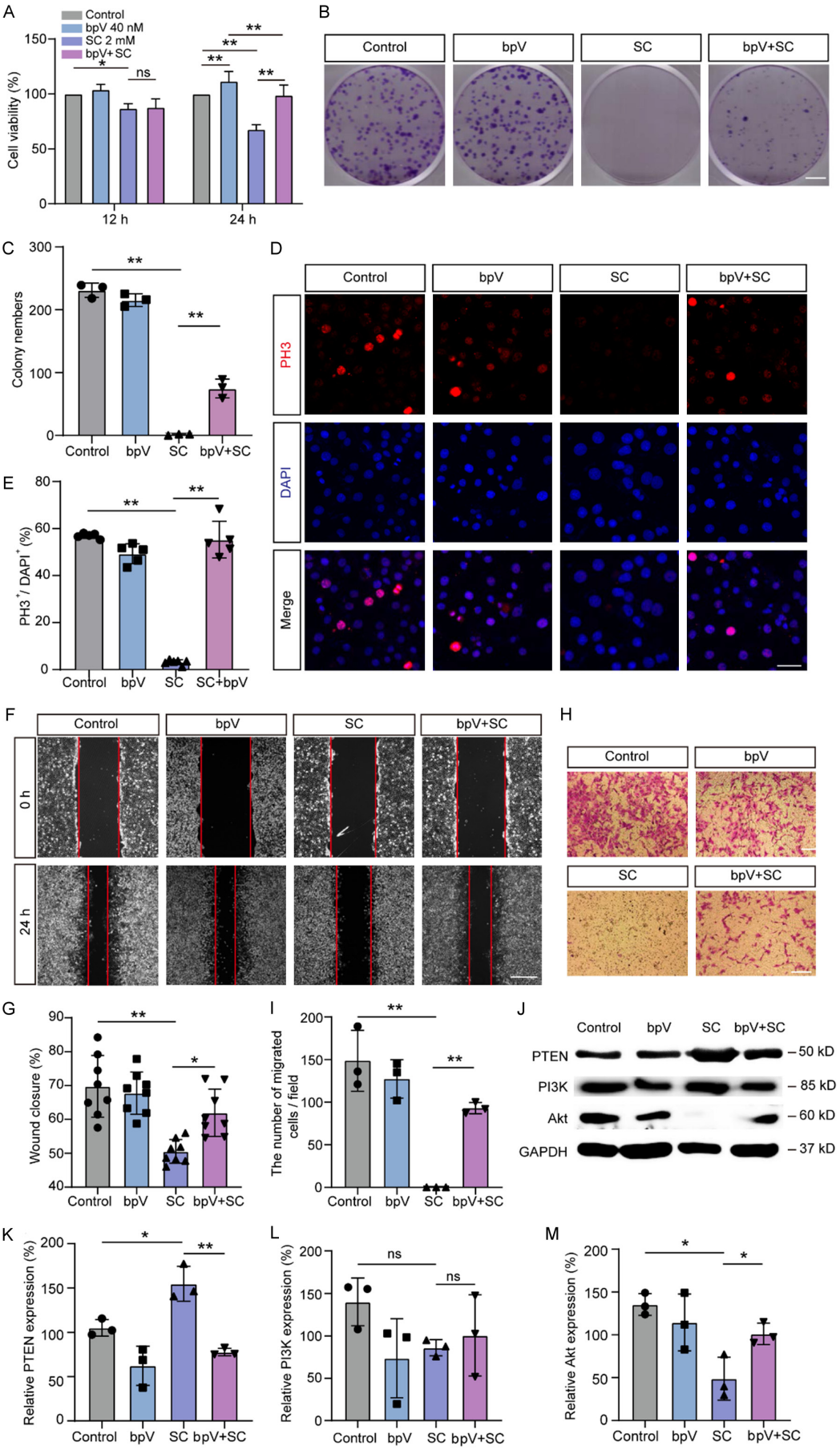
A
Control
bpV 40 nM
SC 2 mM
bpV+SC
Cell viability (%)
12 h
24 h
B
Control
bpV
SC
bpV+SC
C
Colony nembers
D
PH3
DAPI
Merge
E
PH3+/ DAPI+ (%)
SC+bpV
F
0 h
24 h
H
G
Wound closure (%)
I
The number of migrated cells / field
J
PTEN
PI3K
Akt
GAPDH
50 kD
85 kD
60 kD
37 kD
K
Relative PTEN expression (%)
L
Relative PI3K expression (%)
M
Relative Akt expression (%)

Figure 4. Inhibition of PTEN by bpV partially restores the inhibitory effect of sophocarpine on U251 cells. (A) Cell viability of U251 cells upon DMSO, SC, bpV or bpV+SC treatment was measured by CCK-8 assay (normalized to control, n=4, two-way ANOVA). (B) Typical image of U251 cell colony formation upon DMSO, SC, bpV or bpV+SC treatment detected by cell colony-formation assay. Scale bar, 6 mm. (C) Statistical analysis of the number of cell colonies as shown in (B) (n=3, one-way ANOVA). (D) Immunofluorescence staining analysis of PH3 expression of U251 cells upon DMSO, SC, bpV or bpV+SC treatment. Scale bar, 50 μm. (E) Statistical analysis of the $PH3^+/DAPI^+$ cell percentages as shown in (D) (n=5, one-way ANOVA). (F) Wound closure of U251 cells upon DMSO, SC, bpV or bpV+SC treatment was detected by wound healing assay. Scale bar, 150 μm. (G) Wound closure ratios were statistically analyzed as shown in (F) (n=8, one-way ANOVA). (H) Transwell assay detected the migrated cells of U251 upon DMSO, SC, bpV or bpV+SC treatment. Scale bar, 250 μm. (I) Statistical analysis of the migrated cells as shown in (H) (n=3, one-way ANOVA). (J) Western blot analysis of PTEN, PI3K and Akt of U251 cells upon DMSO, SC, bpV or bpV+SC treatment. (K-M) Statistical analysis of the relative expression level of proteins detected in (J) (n=3, one-way ANOVA). Data were represented as mean ± SD, $^*P < 0.05$; $^{**}P < 0.01$.

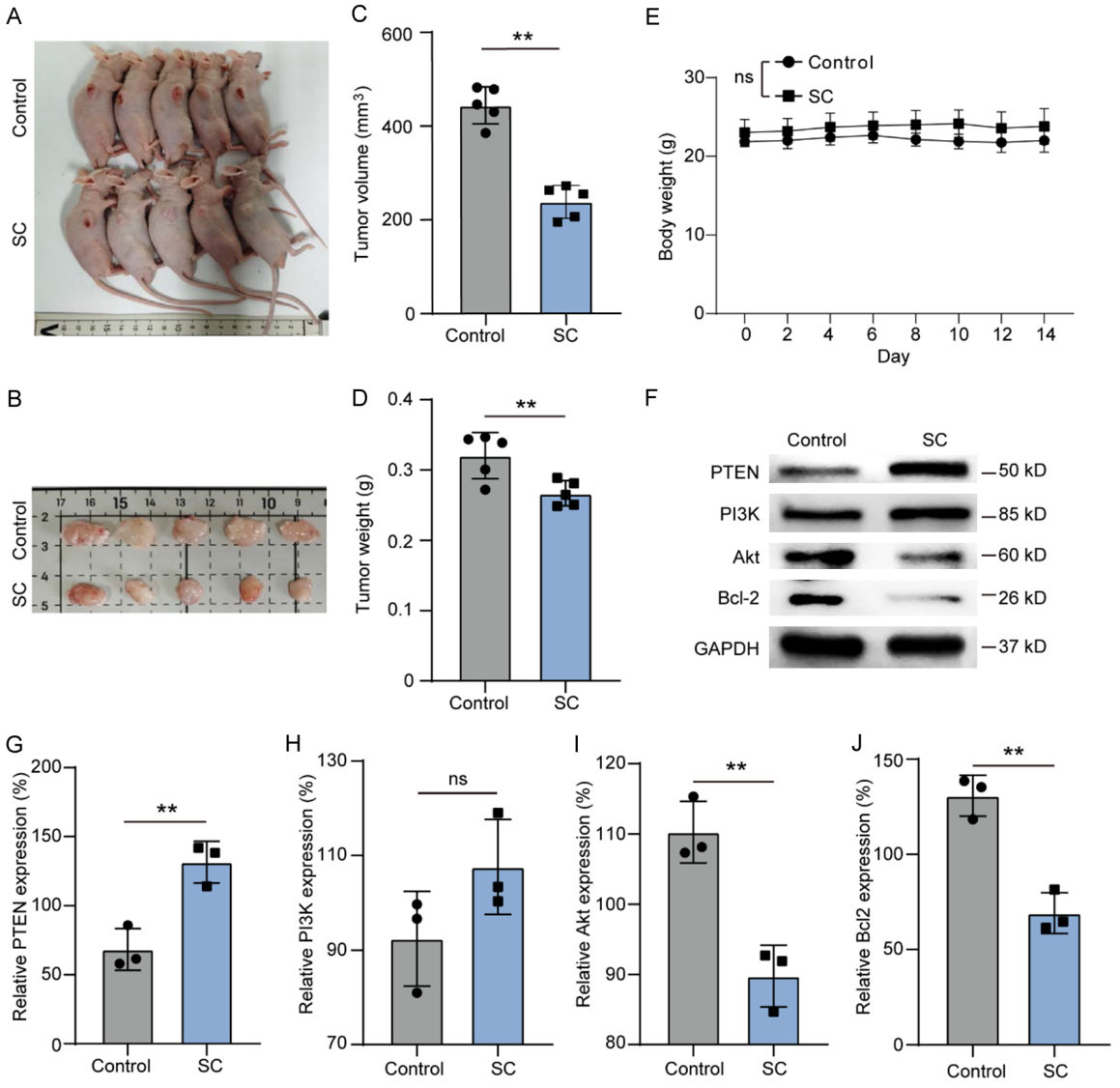

Figure 5. Sophocarpine regresses U251 subcutaneous xenografts growth *in vivo* via PTEN/PI3K/Akt axis. (A, B) Representative result of U251 subcutaneous xenografts in control group and SC group. (C, D) Tumor volumes (C) and tumor weights (D) were calculated and statistically analyzed (n=5, *t*-test). (E) Body weight of tumor-bearing nude mice was calculated and statistically analyzed (n=5, two-way RM ANOVA). (F) Representative results of western blot analysis of expression in subcutaneous xenografts of two groups. (G-J) The relative expression of PTEN, PI3K, Akt and Bcl-2 were statistically analyzed as shown in (F) (n=3, *t*-test). The results were presented as mean ± SD, $^{**}P < 0.01$.

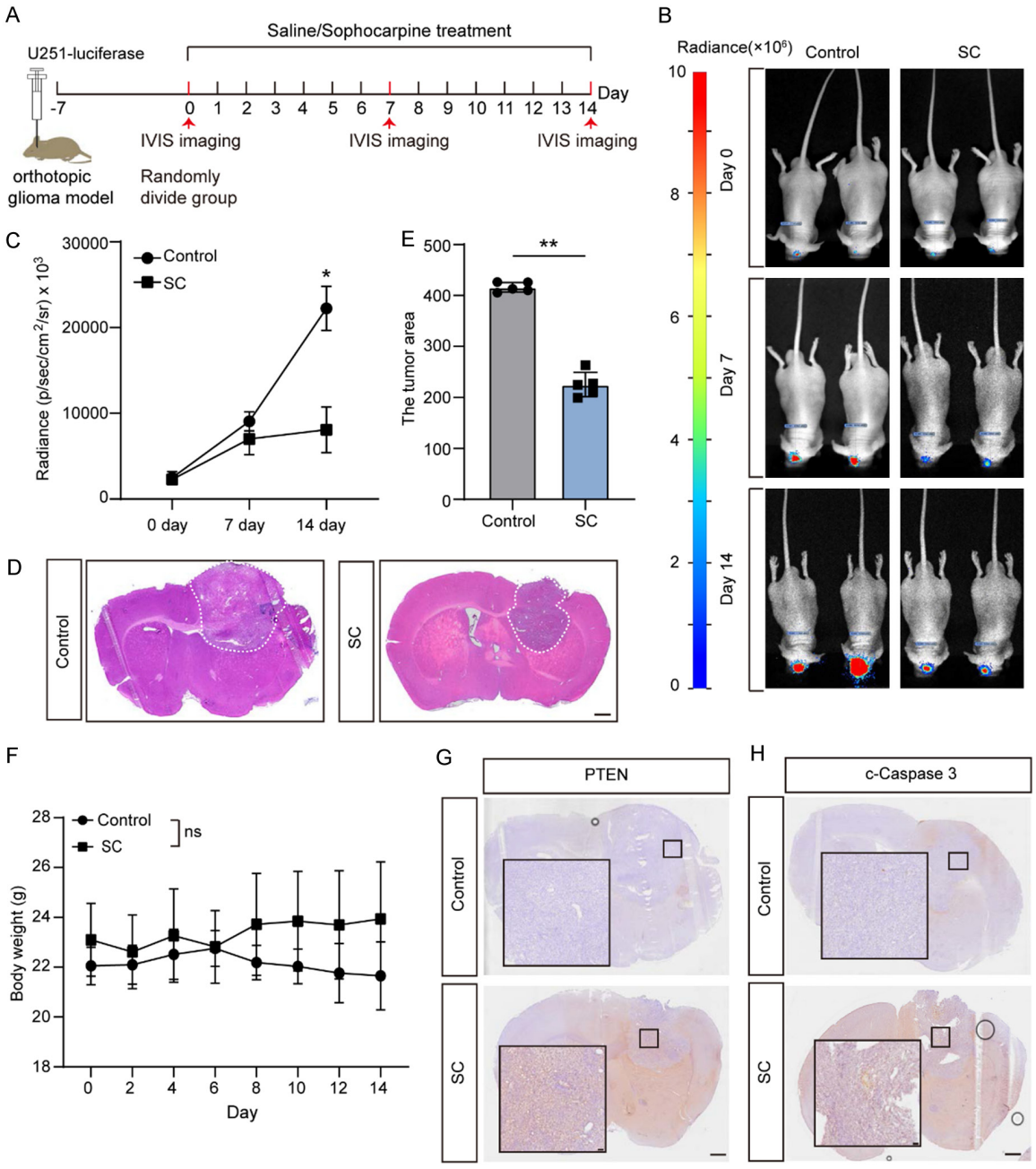

Figure 6. Sophocarpine inhibits GBM tumor growth in orthotopic xenografted tumor model. (A) Schematic diagram of detecting the effects of SC on orthotopic GBM growth. (B) Representative IVIS imaging estimated the therapeutic efficacy of SC on GBM at specified time point as shown in (A). (C) Statistical analysis of the bioluminescence of tumors as shown in (B) (n=5, two-way RM ANOVA). (D) Representative images of HE staining of GBM-bearing mice administrated with saline or SC. Scale bar, 500 μm. (E) The tumor sizes were statistically analyzed as shown in (D) (n=5, *t*-test). (F) Body weights of GBM-bearing mice from (B) were calculated and statistically analyzed (n=5, two-way RM ANOVA). (G, H) Representative image of immunohistochemistry to detect PTEN and cleaved Caspase-3 expression of xenografts in two groups. Scale bar, 500 μm. Data were presented as mean ± SD, $^{*}P < 0.05$; $^{**}P < 0.01$.

we found that sophocarpine significantly regressed the progression of orthotopic GBM compared with control group (**Figure 6B-E**). Besides, body weight of tumor-bearing mice from two groups were also recorded every two days and the result showed that sophocarpine had no impact on their body weight (**Figure 6F**). In addition, immunohistochemistry result

showed that sophocarpine significantly upregulated PTEN and cleaved Caspase-3 expression, indicating that sophocarpine inhibited orthotopic U251 xenografted tumor growth via upregulating of PTEN and inducing cell apoptosis of GBM, which were consistent with the *in vitro* result and *in vivo* result of subcutaneous U251 xenografts in nude mice (**Figure 6G**, **6H**). As shown in Figure S3B, there were also no obviously histological differences in the main organs of tumor-bearing mice treated daily with sophocarpine for two weeks. Taken together, these results suggested that sophocarpine significantly inhibited GBM growth *in vivo*.

Discussion

In the present study, we found a tetracyclic quinazoline alkaloid, sophocarpine, that derived from *Sophora alopecuroides* L., could significantly inhibit the viability, proliferation, migration of GBM cells, and induce the cell cycle arrest in G0/G1 phase and cell apoptosis *in vitro*, as well as inhibit the tumor growth *in vivo*. Molecular investigation revealed that sophocarpine upregulated the expression of PTEN and downregulated PI3K/Akt signaling to impede the progression of GBM (**Figure 7**).

The highly malignant phenotype of GBM is benefit from its characteristics in at least two aspects, fast proliferation rate and strong metastatic ability. The rapid growth of tumor squeezes the surrounding normal brain tissue, and the absence of a clear boundary between the invading tumor cells with the surrounding normal cells makes it difficult to achieve effective resection, usually resulting in rapid recurrence after surgery. Therefore, we first examined the effect of sophocarpine on the viability, proliferation and migration of GBM cells. As a result, CCK8 assay, cell colony-formation and PH3-immunoflurescence assay showed that sophocarpine could significantly inhibit the proliferation of U251 and C6 cells (**Figures 1B-F** and S1A-E). Besides, we also concluded that the migration ability of GBM cells was reduced from wound healing and transwell assays (**Figures 1G-M** and S1F-I). Cell growth is precisely regulated by the cell cycle and cell cycle arrest may result in cell apoptosis. Previous study reported that sophocarpine could block cell cycle at the G0/G1 phase of hepatocellular carcinoma [14] and induce cell apoptosis in gastric cancer [15]. In this study, flow cytometry analysis observed that the ratio of U251 cells in G0/G1 phase was increased (**Figure 2A**, **2B**), as well as the increased proportion of apoptotic cells (**Figure 2F**, **2G**) after sophocarpine treatment. We also noticed that, Cyclin D1 and Cyclin B1, which were involved in regulating cell cycle progression, were downregulated with sophocarpine (**Figure 2C-E**). Besides, the upregulation of P53 and cleaved Caspase-3 accompanied with downregulated Bcl2 also meant the promoted cell apoptosis by sophocarpine (**Figure 2H-K**).

PTEN, also named MMAC1 (mutated in multiple advanced cancers) or TEP1 (TGFβ-regulated and epithelial cell-enriched phosphatase) before, was identified as a tumor suppressor located on chromosome 10q23 in 1997, and often absent or mutated in GBM [18, 19, 21, 32]. PTEN contains motifs homology to the protein tyrosine phosphatase, as well as sequences similarity with the chicken cytoskeletal tensin and bovine auxilin [18, 19]. Protein tyrosine phosphatases possess the ability to resist tyrosine phosphorylation of specific protein tyrosine kinases involved in oncogenesis, and evidences have shown that PTEN is a dual-specificity phosphatase with its phosphatase enzymatic activity required for suppressing tumor [21]. Further, there is increasing evidence showing that PTEN acts as a vital tumor suppressor mainly depends on its lipid phosphatase activity to dephosphorylate PIP3, an important lipid second messenger, into PIP2, thus antagonizing the PI3K/Akt signaling pathway [28, 29]. Previous studies found that PTEN and Akt signaling were associated with sophocarpine to prevent the progression of cancer [14, 15, 17]. However, it remains unknown whether sophocarpine performed anti-GBM effects via targeting PTEN/PI3K/Akt signaling. In our study, we found that sophocarpine significantly upregulated PTEN in both transcription and translation level (**Figure 3A-C**). Meanwhile, both the expression of Akt and p-Akt (Thr308) were downregulated in sophocarpine group, but without influencing the PI3K level (**Figure 3B**, **3D-G**). Furthermore, inhibiting PTEN by bpV could rescue the inhibitory effect of cell viability, proliferation and migration on U251 cells by sophocarpine (**Figure 4**).

Finally, by using subcutaneous and orthotopic GBM xenograft model established in BALB/c nude mice, we observed the inhibition of tumor

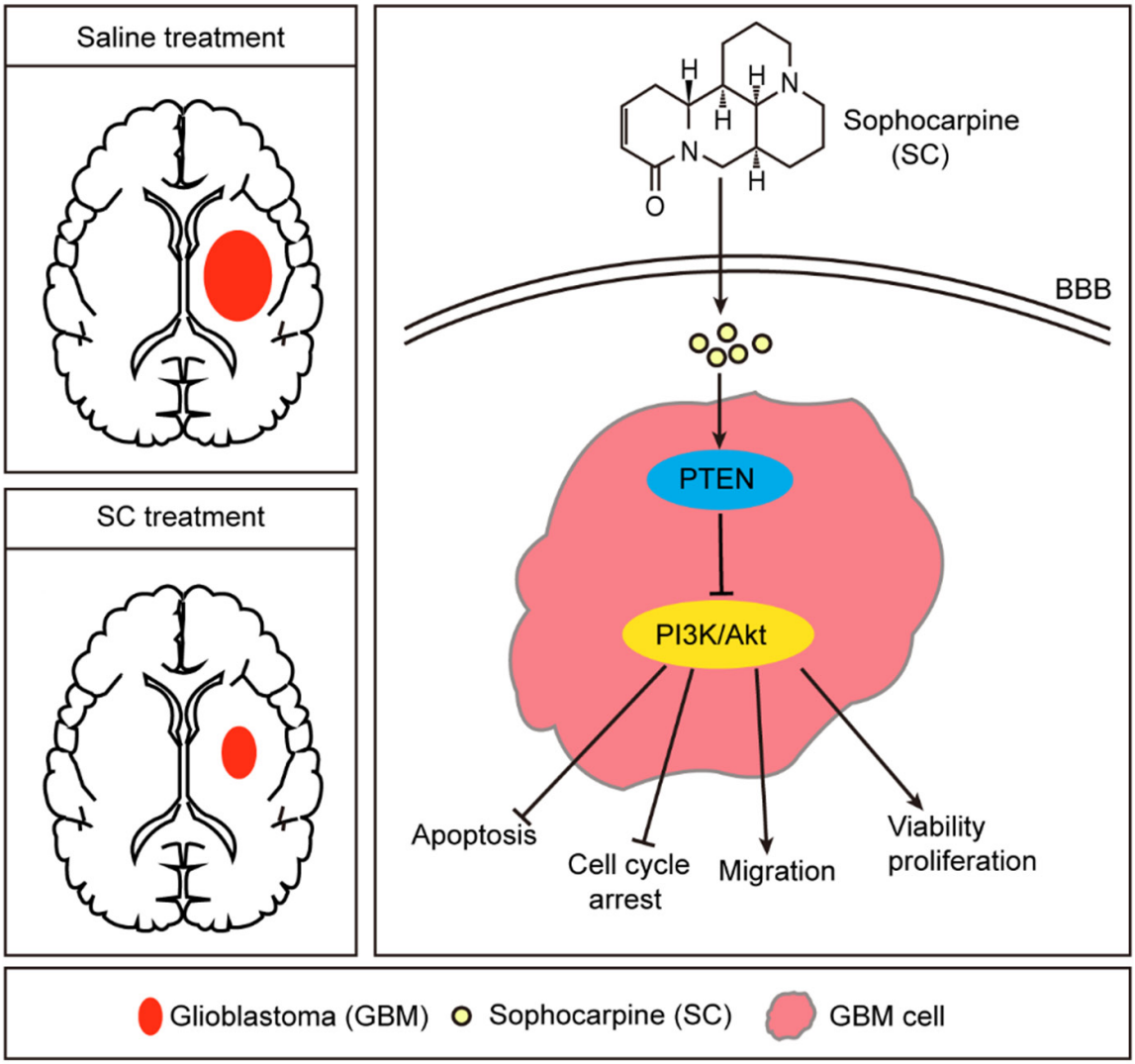

Figure 7. Sophocarpine impedes GBM progression through PTEN/PI3K/Akt axis. SC performs anti-GBM effects both in *in vitro* and *in vivo*. On cellular and molecular level, by upregulating PTEN and downregulating PI3K/Akt signaling, SC suppresses GBM cell viability, proliferation, migration, arrests GBM cell cycle in G0/G1 phase and promotes their apoptosis.

growth with sophocarpine *in vivo*, and the inhibitory effect was also indicated to be associated with PTEN/PI3K/Akt signaling (**Figures 5** and **6**). This is consistent to our network pharmacological analysis which suggested that sophocarpine was tightly associated with PI3K/Akt signaling pathway in GBM (data not shown). Still, we noticed that the rescue effect of bpV on the GBM growth inhibition was partial, indicating that there exist other undiscovered targets involved in the toxicity for sophocarpine in GBM. Besides, phosphorylation at both Thr308 and Ser473 sites of Akt represents the maximal Akt activation [33], however, Akt-Thr308, which we detected in our study, was sufficient for Akt activation [34].

Besides, although the concentration of sophocarpine used to inhibit the growth of GBM cells is relatively high with millimolar level, still, it has no obvious toxic effect on primary cultured normal astrocytes (Figure S2). Such concentration level of sophocarpine was also used in other cancers [16, 17]. Moreover, matrine, another alkaloid in *Sophora* plants, also has the effect of being used in millimolar level to reduce the proliferation of cancer cells [35, 36] but gentle to normal cells [36]. However, 35 mg/kg, the

concentration used to effectively impede the growth of GBM tumor *in vivo* is relatively low, and as expected, without toxicity to the tumor-bearing mice (**Figures 5E**, **6F** and S3). On the one hand, it suggested that sophocarpine might possess certain ability to cross the blood-brain barrier to reach and affect the intracranial tumor, on the other hand, it was possible that the metabolites of sophocarpine metabolism *in vivo* also exhibited potential anti-tumor effects and blood-brain barrier permeability, and which needed further investigation.

Conclusions

In conclusion, we found sophocarpine, a natural tetracyclic quinazoline alkaloid derived from an anti-tumor traditional Chinese medicine, can significantly suppress the growth of GBM both *in vitro* and *in vivo*. The molecular investigation revealed that sophocarpine could upregulate the GBM tumor suppressor PTEN expression and subsequently downregulate PI3K/Akt signaling. These results suggest that sophocarpine is a promising natural therapy for GBM.

Acknowledgements

This project was supported by the National Natural Science Foundation of China (No. 82-103210) and the Research Start-up Project by Hangzhou Normal University (No. 4125C50-220204106).

Disclosure of conflict of interest

None.

Abbreviations

GBM, Glioblastoma multiforme; SC, Sophocarpine; PTEN, Phosphatase and tensin homolog absent on chromosome 10; PI3K, Phosphatidylinositol 3-kinase; PIP2, Phosphatidylinositol-4,5-bisphosphate; PIP3, Phosphatidylinositol-3,4,5-trisphosphate; Akt, Serine/threonine kinase; PH3, Phospho-Histone H3; Bcl-2, B-cell lymphoma-2; P53, Protein 53 or tumor protein 53; TGFβ, Transforming growth factor beta.

Address correspondence to: Yuanyuan Jiang, School of Pharmacy, Hangzhou Normal University, Hangzhou 311121, Zhejiang, China. E-mail: jiangyuanyuan@hznu.edu.cn

References

[1] Krex D, Klink B, Hartmann C, von Deimling A, Pietsch T, Simon M, Sabel M, Steinbach JP, Heese O, Reifenberger G, Weller M and Schackert G; German Glioma Network. Long-term survival with glioblastoma multiforme. Brain 2007; 130: 2596-2606.

[2] Stupp R, Mason WP, van den Bent MJ, Weller M, Fisher B, Taphoorn MJ, Belanger K, Brandes AA, Marosi C, Bogdahn U, Curschmann J, Janzer RC, Ludwin SK, Gorlia T, Allgeier A, Lacombe D, Cairncross JG, Eisenhauer E and Mirimanoff RO; European Organisation for Research and Treatment of Cancer Brain Tumor and Radiotherapy Groups; National Cancer Institute of Canada Clinical Trials Group. Radiotherapy plus concomitant and adjuvant temozolomide for glioblastoma. N Engl J Med 2005; 352: 987-996.

[3] Lu JJ, Bao JL, Chen XP, Huang M and Wang YT. Alkaloids isolated from natural herbs as the anticancer agents. Evid Based Complement Alternat Med 2012; 2012: 485042.

[4] Khalighi-Sigaroodi F, Ahvazi M, Hadjiakhoondi A, Taghizadeh M, Yazdani D, Khalighi-Sigaroodi S and Bidel S. Cytotoxicity and antioxidant activity of 23 plant species of leguminosae family. Iran J Pharm Res 2012; 11: 295-302.

[5] Luo H and Zhou D. Introduction of the commonly used as anti-tumor herbs. New Journal of Tranditional Chinese Medicine 1978.

[6] Li XM, Li LZ, Chen SL, Qiu XH, Yu YH, Pan DX, Zou LL, Yang ZL and Han YS. Inhibitory effects of sophocarpine on animal tumors. Zhongguo Yao Li Xue Bao 1984; 5: 125-130.

[7] Gao Y, Jiang W, Dong C, Li C, Fu X, Min L, Tian J, Jin H and Shen J. Anti-inflammatory effects of sophocarpine in LPS-induced RAW 264.7 cells via NF-kappaB and MAPKs signaling pathways. Toxicol In Vitro 2012; 26: 1-6.

[8] Wang XJ, Deng HZ, Jiang B and Yao H. The natural plant product sophocarpine ameliorates dextran sodium sulfate-induced colitis in mice by regulating cytokine balance. Int J Colorectal Dis 2012; 27: 575-581.

[9] Jiang Z, Meng Y, Bo L, Wang C, Bian J and Deng X. Sophocarpine attenuates LPS-induced liver injury and improves survival of mice through suppressing oxidative stress, inflammation, and apoptosis. Mediators Inflamm 2018; 2018: 5871431.

[10] Qavi HB, Wyde PR and Khan MA. In vitro Inhibition of HHV-6 replication by sophocarpines. Phytother Res 2002; 16: 154-156.

[11] Jin Z, Yang L, Ding G, Yang G, Han Y, Zhang X and Li W. Sophocarpine against enterovirus 71 in vitro. Exp Ther Med 2017; 14: 3792-3797.

[12] Yifeng M, Bin W, Weiqiao Z, Yongming Q, Bing L and Xiaojie L. Neuroprotective effect of sophocarpine against transient focal cerebral ischemia via down-regulation of the acid-sensing ion channel 1 in rats. Brain Res 2011; 1382: 245-251.
[13] Ye JY, Hao Q, Zong Y, Shen Y, Zhang Z and Ma C. Sophocarpine attenuates cognitive impairment and promotes neurogenesis in a mouse model of Alzheimer's disease. Neuroimmunomodulation 2021; 28: 166-177.
[14] Zhang PP, Wang PQ, Qiao CP, Zhang Q, Zhang JP, Chen F, Zhang X, Xie WF, Yuan ZL, Li ZS and Chen YX. Differentiation therapy of hepatocellular carcinoma by inhibiting the activity of AKT/GSK-3beta/beta-catenin axis and TGF-beta induced EMT with sophocarpine. Cancer Lett 2016; 376: 95-103.
[15] Huang Y, Chen X, Guo G, Guo W, Ma Q and Yuan J. Sophocarpine inhibits the growth of gastric cancer cells via autophagy and apoptosis. Front Biosci (Landmark Ed) 2019; 24: 616-627.
[16] Wang Q, Wang T, Zhu L, He N, Duan C, Deng W, Zhang H and Zhang X. Sophocarpine inhibits tumorgenesis of colorectal cancer via down-regulation of MEK/ERK/VEGF pathway. Biol Pharm Bull 2019; 42: 1830-1838.
[17] Liu W, Zhang B, Chen G, Wu W, Zhou L, Shi Y, Zeng Q, Li Y, Sun Y, Deng X and Wang F. Targeting miR-21 with sophocarpine inhibits tumor progression and reverses epithelial-mesenchymal transition in head and neck cancer. Mol Ther 2017; 25: 2129-2139.
[18] Li J, Yen C, Liaw D, Podsypanina K, Bose S, Wang SI, Puc J, Miliaresis C, Rodgers L, McCombie R, Bigner SH, Giovanella BC, Ittmann M, Tycko B, Hibshoosh H, Wigler MH and Parsons R. PTEN, a putative protein tyrosine phosphatase gene mutated in human brain, breast, and prostate cancer. Science 1997; 275: 1943-1947.
[19] Steck PA, Pershouse MA, Jasser SA, Yung WK, Lin H, Ligon AH, Langford LA, Baumgard ML, Hattier T, Davis T, Frye C, Hu R, Swedlund B, Teng DH and Tavtigian SV. Identification of a candidate tumour suppressor gene, MMAC1, at chromosome 10q23.3 that is mutated in multiple advanced cancers. Nat Genet 1997; 15: 356-362.
[20] Teng DH, Hu R, Lin H, Davis T, Iliev D, Frye C, Swedlund B, Hansen KL, Vinson VL, Gumpper KL, Ellis L, El-Naggar A, Frazier M, Jasser S, Langford LA, Lee J, Mills GB, Pershouse MA, Pollack RE, Tornos C, Troncoso P, Yung WK, Fujii G, Berson A, Steck PA, et al. MMAC1/PTEN mutations in primary tumor specimens and tumor cell lines. Cancer Res 1997; 57: 5221-5225.
[21] Myers MP, Stolarov JP, Eng C, Li J, Wang SI, Wigler MH, Parsons R and Tonks NK. P-TEN, the tumor suppressor from human chromosome 10q23, is a dual-specificity phosphatase. Proc Natl Acad Sci U S A 1997; 94: 9052-9057.
[22] Furnari FB, Lin H, Huang HS and Cavenee WK. Growth suppression of glioma cells by PTEN requires a functional phosphatase catalytic domain. Proc Natl Acad Sci U S A 1997; 94: 12479-12484.
[23] Tamura M, Gu J, Matsumoto K, Aota S, Parsons R and Yamada KM. Inhibition of cell migration, spreading, and focal adhesions by tumor suppressor PTEN. Science 1998; 280: 1614-1617.
[24] Maehama T and Dixon JE. The tumor suppressor, PTEN/MMAC1, dephosphorylates the lipid second messenger, phosphatidylinositol 3,4,5-trisphosphate. J Biol Chem 1998; 273: 13375-13378.
[25] Stephens LR, Jackson TR and Hawkins PT. Agonist-stimulated synthesis of phosphatidylinositol(3,4,5)-trisphosphate: a new intracellular signalling system? Biochim Biophys Acta 1993; 1179: 27-75.
[26] Vivanco I and Sawyers CL. The phosphatidylinositol 3-kinase AKT pathway in human cancer. Nat Rev Cancer 2002; 2: 489-501.
[27] Chautard E, Ouedraogo ZG, Biau J and Verrelle P. Role of Akt in human malignant glioma: from oncogenesis to tumor aggressiveness. J Neurooncol 2014; 117: 205-215.
[28] Das S, Dixon JE and Cho W. Membrane-binding and activation mechanism of PTEN. Proc Natl Acad Sci U S A 2003; 100: 7491-7496.
[29] Vazquez F, Matsuoka S, Sellers WR, Yanagida T, Ueda M and Devreotes PN. Tumor suppressor PTEN acts through dynamic interaction with the plasma membrane. Proc Natl Acad Sci U S A 2006; 103: 3633-3638.
[30] Lambert AW, Pattabiraman DR and Weinberg RA. Emerging biological principles of metastasis. Cell 2017; 168: 670-691.
[31] Tang W, Lin D, Chen M, Li Z, Zhang W, Hu W and Li F. PTEN-mediated mitophagy and APE1 overexpression protects against cardiac hypoxia/reoxygenation injury. In Vitro Cell Dev Biol Anim 2019; 55: 741-748.
[32] Li DM and Sun H. TEP1, encoded by a candidate tumor suppressor locus, is a novel protein tyrosine phosphatase regulated by transforming growth factor beta. Cancer Res 1997; 57: 2124-2129.
[33] Alessi DR, James SR, Downes CP, Holmes AB, Gaffney PR, Reese CB and Cohen P. Character-

ization of a 3-phosphoinositide-dependent protein kinase which phosphorylates and activates protein kinase Balpha. Curr Biol 1997; 7: 261-269.

[34] Stokoe D, Stephens LR, Copeland T, Gaffney PR, Reese CB, Painter GF, Holmes AB, McCormick F and Hawkins PT. Dual role of phosphatidylinositol-3,4,5-trisphosphate in the activation of protein kinase B. Science 1997; 277: 567-570.

[35] Dai ZJ, Gao J, Ji ZZ, Wang XJ, Ren HT, Liu XX, Wu WY, Kang HF and Guan HT. Matrine induces apoptosis in gastric carcinoma cells via alteration of Fas/FasL and activation of caspase-3. J Ethnopharmacol 2009; 123: 91-96.

[36] Liu T, Song Y, Chen H, Pan S and Sun X. Matrine inhibits proliferation and induces apoptosis of pancreatic cancer cells in vitro and in vivo. Biol Pharm Bull 2010; 33: 1740-1745.

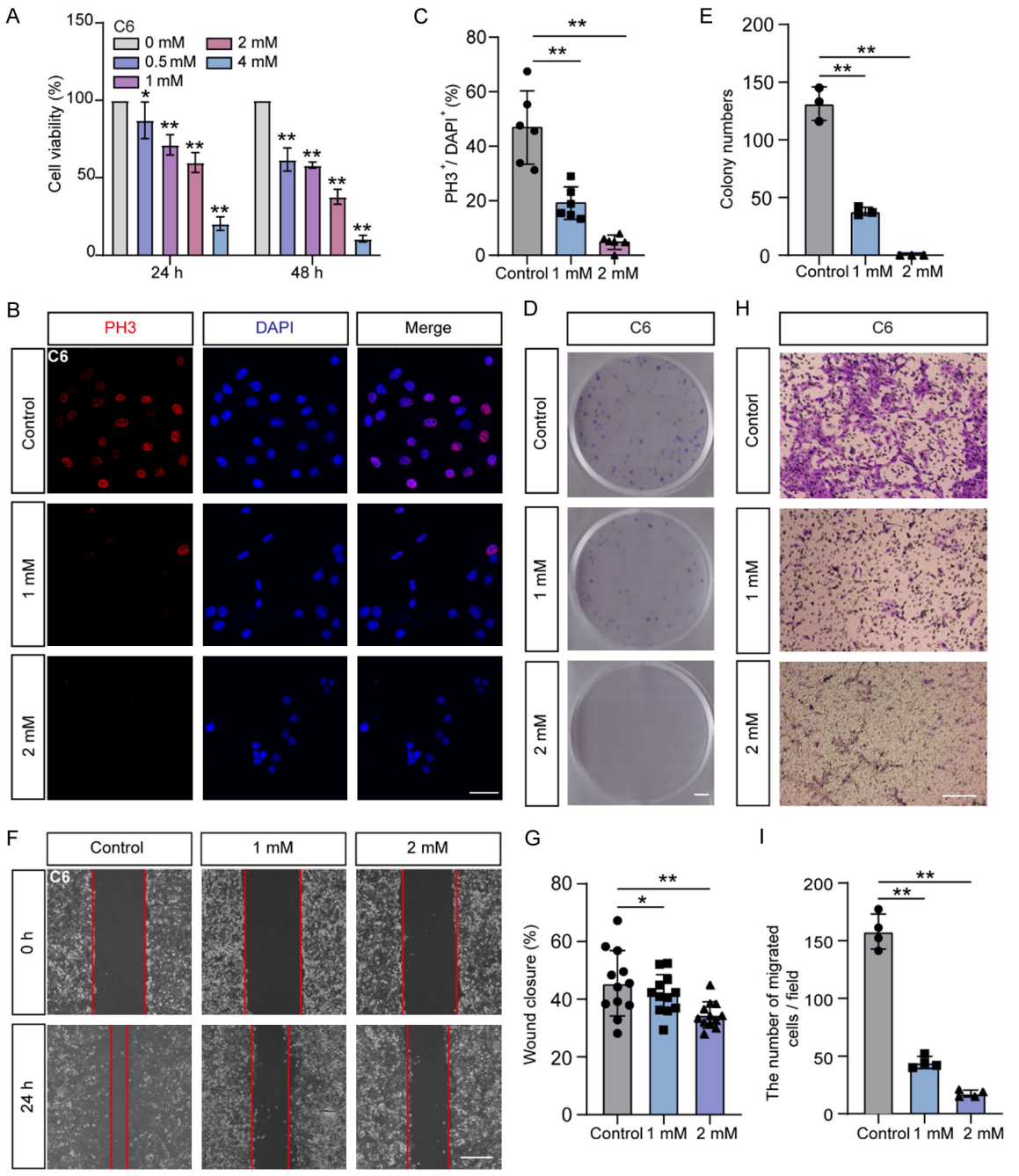

Figure S1. Sophocarpine inhibits the viability, proliferation and migration of C6 cells. (A) Cell viability of C6 cells upon gradient concentrations of SC treatment were measured by CCK-8 assay (normalized to control, n=4, two-way ANOVA). (B) Representative images of PH3 immunostaining of C6 cells upon DMSO, 1 mM or 2 mM SC treatment. Scale bar, 50 μm. (C) Statistical analysis of $PH3^+$ cell percentages as shown in (B) (n=6, one-way ANOVA). (D) Representative images of C6 cell colony formation upon DMSO, 1 mM or 2 mM SC treatment detected by cell colony-formation assay. Scale bar, 5 mm. (E) Statistically analysis of cell colony numbers as shown in (D) (n=3, one-way ANOVA). (F) Wound closure of C6 cells upon DMSO, 1 mM or 2 mM SC treatment detected by wound healing assay. Scale bar, 150 μm. (G) The wound closure ratios were statistically analyzed as shown in (F) (n=12, one-way ANOVA). (H) The migrated C6 cells upon DMSO, 1 mM or 2 mM SC treatment detected by transwell assay. Scale bar, 250 μm. (I) Statistical analysis of the migrated cells as shown in (H) (n=4, one-way ANOVA). The results were presented as mean ± SD, $^*P < 0.05$; $^{**}P < 0.01$.

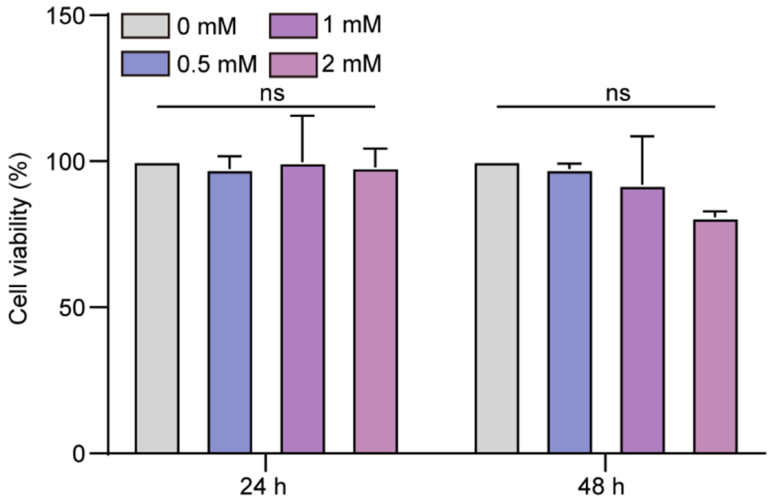

Figure S2. Sophocarpine has no toxicity to the primary cultured astrocytes from C57BL/6J mice. The viability of primary cultured astrocytes upon SC concentration gradient were measured by CCK8 assay (normalized to control, n=4, two-way ANOVA). Data were presented as mean ± SD.

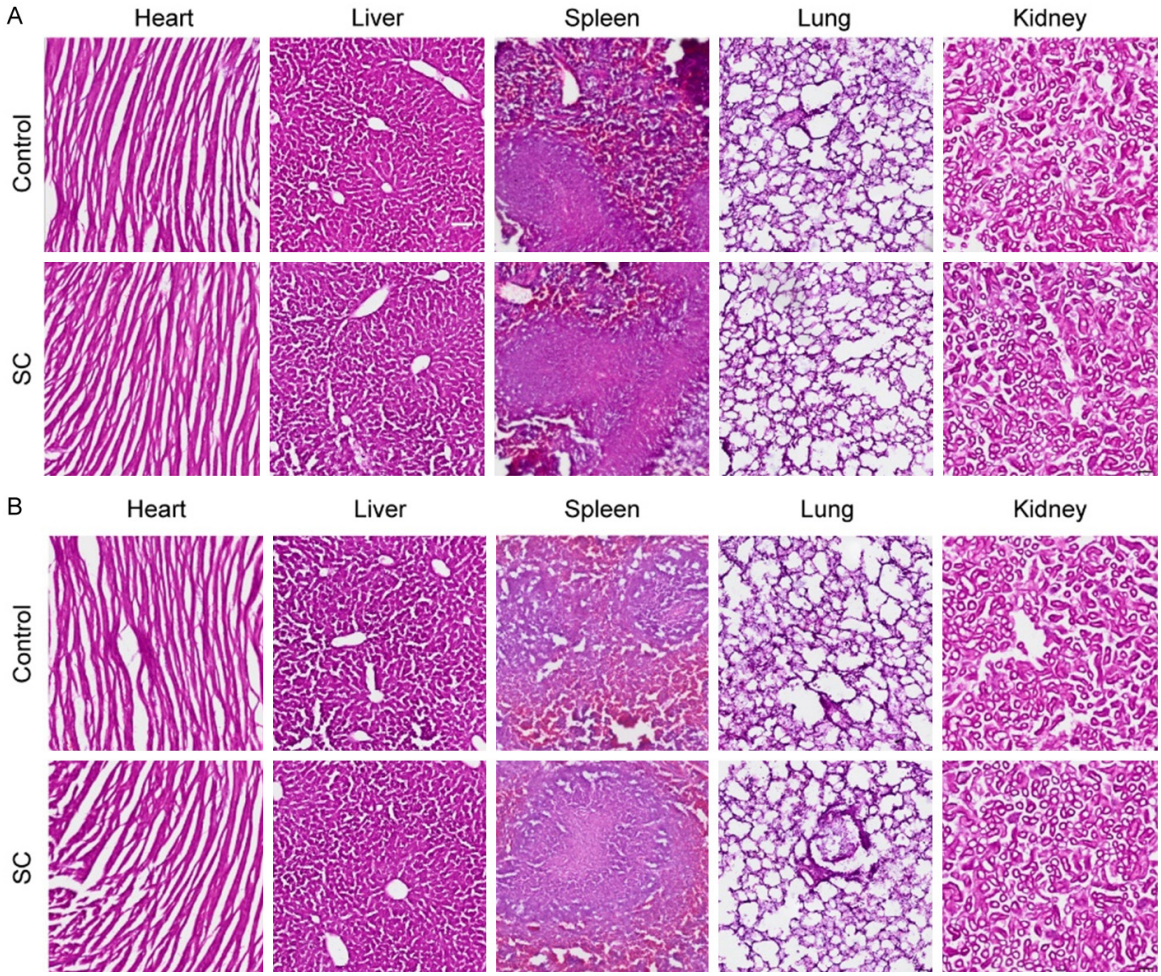

Figure S3. Sophocarpine has no significant toxic effects on main organs of GBM-bearing mice. A. Typical images of HE staining for frozen sections from major organs in saline-treated and SC-treated U251 subcutaneous xenograft tumor-bearing mice. B. Typical images of HE staining for frozen sections from major organs in saline-treated and SC-treated U251 orthotopic tumor-bearing mice. Scale bar, 100 μm.